Binding of L-kynurenine to X. campestris tryptophan 2,3-dioxygenase

Binding of L-kynurenine to *X. campestris* tryptophan 2,3-dioxygenase

Jaswir Basran[a], Elizabeth S. Booth[b], Laura P. Campbell[c], Sarah J. Thackray[c], Mehul H. Jesani[d], Jonathan Clayden[d], Peter C.E. Moody[a], Christopher G. Mowat[c], Hanna Kwon[d,*] and Emma L. Raven[d,*]

[a] *Department of Molecular and Cell Biology and Leicester Institute of Structural and Chemical Biology, University of Leicester, Leicester, LE1 9HN, UK*
[b] *Department of Chemistry and Leicester Institute of Structural and Chemical Biology, University of Leicester, Leicester, LE1 7RH, UK.*
[c] *EastChem School of Chemistry, University of Edinburgh, David Brewster Road, Edinburgh, EH9 3FJ, UK.*
[d] *School of Chemistry, University of Bristol, Cantock's Close, Bristol, BS8 1TS, UK.*

**To whom correspondence should be addressed. E-mail: hanna.kwon@bristol.ac.uk and emma.raven@bristol.ac.uk.*

Keywords: heme, tryptophan 2,3-dioxygenase, kynurenine, cyanide.

Abbreviations: TDO – tryptophan 2,3-dioxygenase; NFK – *N*-formylkynurenine; IDO – indoleamine 2,3-dioxygenase.

Abstract
The kynurenine pathway is the major route of tryptophan metabolism. The first step of this pathway is catalysed by one of two heme-dependent dioxygenase enzymes – tryptophan 2,3-dioxygenase (TDO) and indoleamine 2,3-dioxygenase (IDO) – leading initially to the formation of *N*-formylkynurenine (NFK). In this paper, we present a crystal structure of a bacterial TDO from *X. campestris* in complex with L-kynurenine, the hydrolysed product of NFK. L-kynurenine is bound at the active site in a similar location to the substrate (L-Trp). Hydrogen bonding interactions with Arg117 and the heme 7-propionate anchor the L-kynurenine molecule into the pocket. A mechanism for the hydrolysis of NFK in the active site is presented.

1. Introduction

The heme-dependent dioxygenases tryptophan 2,3-dioxygenase (TDO) and indoleamine 2,3-dioxygenase (IDO) catalyse the insertion of both atoms of molecular oxygen into L-tryptophan (L-Trp) to form *N*-formylkynurenine (NFK) in the first and rate-limiting step in the kynurenine pathway [1-3], Fig. 1. This pathway processes approximately 95% of dietary tryptophan in humans and is responsible for the production of the essential cofactor nicotinamide adenine dinucleotide [4, 5]. In addition to this crucial function, the kynurenine pathway is also important in the pathophysiology of several diseases. Increased levels of certain metabolites, such as quinolinic acid and L-kynurenine, can lead to conditions such as multiple sclerosis, AIDS-related dementia and ischemic brain injury [6, 7]. Furthermore, some kynurenine pathway metabolites can contribute to immunosuppressive pathways and suppress proliferation (and even cause apoptosis) of T cells, although the mechanisms of action of such metabolites are unknown [8, 9].

There is no information on the binding of L-kynurenine in either an IDO or a TDO. Here we present a crystal structure of a variant *X. campestris* TDO (H55S variant) in complex with L-kynurenine, the hydrolysed product of NFK.

2. Materials and Methods

Protein Expression and Purification. Full-length wild type *X. campestris* TDO (*Xc*TDO) and the H55S mutant were over-expressed and purified as described previously [10, 11], with the exception that cultures were grown at 37 ºC in *Escherichia coli* BL21(DE3) Gold cells in order to increase protein yield. An additional purification step was added to improve the purity of the H55S mutant enzyme. After Ni-NTA chromatography, the protein was applied to a Superdex 200 size exclusion column (50 mM Tris-HCl pH 8.0, 500 mM NaCl) and the peak corresponding to tetrameric protein (~136 kDa) was collected, concentrated and exchanged into 50 mM Tris-HCl buffer pH 8.0. Protein and heme concentrations were determined by the Bradford and pyridine hemochromagen methods respectively [12, 13], and using published absorption coefficients [14].

Steady State Kinetics. For steady state activity measurements, the formation of NFK was monitored at 321nm ($\varepsilon = 3750\ M^{-1}cm^{-1}$) as a function of time. Reactions were performed with 1-3 μM *Xc*TDO or H55S in 50 mM Tris-HCl pH 8.0 at 25 °C and were initiated by addition of 2 mM L-tryptophan.

Protein Crystallography. Crystallisation of the H55S variant of *Xc*TDO was carried out by the hanging drop vapour diffusion method at 18 ºC in Linbro plates. Crystals were grown with well solutions comprising 9-10 % (w/v) PEG 1000, 80 mM MES (2-(N-morpholino)ethanesulfonic acid) pH 6.3, 20 mM bicine (N,N-bis(2-hydroxyethyl)glycine) pH 9.0, 40 mM $MnCl_2$, 400 mM $MgCl_2$, 8-15 mM sodium cyanide and 25 mM L-Trp. Hanging drops (4 μl final volume) were prepared by adding 2 μl of 8 mg/ml protein (50 mM Tris-HCl pH 8.0, 5 mM EDTA) to 2 μl of the well solution. Red tetragonal shaped crystals appeared after approximately one week, reaching full size after three weeks. Initially, data were collected on these crystals in an attempt to obtain a structure of the H55S/Trp/CN^- ternary complex. However, on refinement no density for a cyanide ligand was observed at the heme iron. To obtain the ternary complex, crystals as prepared above were briefly exposed to mother liquor supplemented with varying concentrations of sodium cyanide (20-70 mM) and 25 % (v/v) glycerol before being flash cooled in liquid nitrogen.

Data Collection and Refinement. The data were collected at ESRF, Grenoble. Data processing and refinements were carried out using CCP4 [15] and PHENIX[16]. Atomic coordinates have been deposited in the Protein Data Bank (PDB ID codes 7P46).

3. Results

A recombinant version of the H55S variant of *Xc*TDO was expressed in *E. coli* and crystallised as stated in the Methods. Data collection and refinement statistics are shown in Table 1. Crystals were found to belong to space group $P2_1$ with cell dimensions of a = 78.09 Å, b = 117.75 Å, c = 138.82 Å, and β = 95.52º. Two tetramers are found in the asymmetric unit.

A previous structure [10] from crystals of *Xc*TDO grown anaerobically in the presence of L-Trp shows the substrate bound in the active site. In this work however (carried out aerobically), the density map shows L-kynurenine, the hydrolysed product of NFK (Fig. 1), in the active site instead (Fig. 2A, B). This is observed in all eight molecules in the unit cell. Apart from the presence of L-kynurenine and cyanide bound to the heme iron, this structure is essentially

identical to the previously published structure of the H55S variant of *Xc*TDO [11]. The final model also includes eight L-tryptophan molecules (one per monomer) bound at the tetramer interface, Fig. 2C, in the same site as observed for all three previously published *Xc*TDO substrate-bound structures [10, 11]. A polypeptide loop (residues Phe250-Val260, which is disordered in the absence of substrate [10], is observed in a closed conformation in the structure, Fig. 2C.

The L-kynurenine is bound to the enzyme through hydrogen bonding interactions, Fig. 2B, that closely reproduce those observed in the structure of the H55S/L-Trp complex, Fig. S1A,B. The carboxylate group of L-kynurenine forms a hydrogen bond to the phenolic group of Tyr113, to the guanidinium moiety of Arg117, and to the heme 7-propionate. The L-kynurenine molecule is further stabilised by van der Waals interactions with residues Phe51, Tyr24, Tyr 27 and Leu28 (not shown). The active site serine 55 residue hydrogen bonds to nearby water, Fig. S1A,B, but does not have any direct interaction with either the substrate (Fig. S1B) or the product (Fig. S1A), unlike the equivalent histidine residue of the wild type protein which hydrogen bonds to the N_1 atom of L-Trp (Fig. S1C).

The binding of L-kynurenine can only be accounted for by turnover of L-Trp in the ferric crystal, leading to formation of NFK and its subsequent hydrolysis to L-kynurenine (Fig. 1). In parallel experiments in solution, we measured slow increases in absorbance at 321 nm, indicative of formation of NFK, on incubation of both ferric *Xc*TDO (k_{cat} = 1 s^{-1}) and ferric H55S (k_{cat} = 0.01 s^{-1}) with L-Trp under normal atmospheric conditions (Fig. 3A,B). Ferrous *Xc*TDO, under conditions of a typical dioxygenase assay using ascorbate, methylene blue and L-Trp, is reported as having k_{cat} = 19.5 s^{-1} and K_M = 114 μM [11].

The exact mechanism for oxidation of L-Trp by the ferric enzyme has not been established, although in the case of human TDO it is dependent on O_2 because no oxidation of L-Trp is observed under anaerobic conditions [17]. Similarly, formation of NFK does not occur during incubation of L-Trp over 5 hours with wild type ferric *Xc*TDO under anaerobic conditions (data not shown) or for H55S, Figure 3C, which suggests that the ferric activity of H55S is O_2-dependent as for human TDO. Note that IDO, unlike the TDOs, cannot oxidise L-Trp in its ferric form [17]. This highlights the differences in the reactivities of the two enzymes, despite the high degree of structural similarity in their active sites.

Experiments in solution also provide some rationalisation for the initial absence of cyanide in the structure presented here, and the need for further soaking with cyanide to produce the ternary complex. In solution, addition of KCN to ferric *Xc*TDO leads to the expected spectral shift of the Soret band to 419 nm, characteristic of the ferric-CN complex (K_D = 47 ± 4 μM for *Xc*TDO and K_D = 3.4 ± 0.1 μM for *Xc*TDO H55S); subsequent binding of Trp causes a slight reduction in the intensity of the 419 nm peak in both cases (not shown). With prolonged incubation of this ferric sample over a period of hours, a clear increase in absorbance at 321 nm was observed, indicating formation of NFK even in the presence of cyanide (Fig. 3D). In agreement with these observations, addition of cyanide to an assay solution of either *Xc*TDO or *Xc*TDO H55S had a minor effect on the rate of NFK formation, Fig. S2A,B. Notably, these observations are in contrast to the behaviour of human TDO, where addition of cyanide to the ferric enzyme either before or during a reaction with L-Trp completely inhibits NFK production, Figure S2C. Ferric *Xc*TDO and *Xc*TDO H55S thus appear to be competent for NFK formation regardless of whether cyanide is present.

Discussion

There are numerous structures for IDO and TDO in the Protein Data Bank, some of which have L-Trp bound, Table 2. The binding orientation of L-kynurenine in the active site of H55S overlays well with that observed for the binding of L-Trp binding in the wild type and H55S enzymes (Fig. 4A) [11, 18]. There is no previously published information on binding of L-kynurenine in a TDO or IDO enzyme, but there is helpful information on human TDO in complex with NFK [19]. There is a close overlay of the L-kynurenine-bound and NFK-bound structures, Fig. 4B. Some hydrogen bonding interactions – to the heme propionate and the active site Arg residue – are conserved between the two, Fig. S3, and presumably will control release of product from the enzyme. These hydrogen bonding interactions between the substrate/product and the enzyme might well control the reactivity of the ternary Michaelis complex in the family of tryptophan dioxygenases [20]. Most of the reported inhibitor structures are for ferric enzymes (Table 2) which, as we show here, can be active towards the substrate (L-Trp).

The binding of L-kynurenine in the active site, as observed in this work, can only be accounted for by turnover of L-Trp in the ferric crystal, leading to formation of NFK and its subsequent hydrolysis to L-kynurenine (Fig. 1). This is consistent with previous work on human TDO [17, 21] and mosquito TDO [22], which can convert L-tryptophan to NFK in the absence of a reductant (albeit at a much lower rate than the ferrous enzyme). There is evidence from other work [23] that substrate (L-Trp) can reduce the ferric enzyme; this remains a possibility here, and would allow O_2 binding and formation of NFK. The subsequent hydrolysis of the unhindered amide group of NFK to L-kynurenine, Figure 1, is known in the chemical literature [24, 25]. A possible mechanism for this *Xc*TDO-catalysed hydrolysis reaction is shown in Figure 5, which could be initiated by attack of any water molecule in the active site. It is significant that the H55S variant of *Xc*TDO has a water molecule ideally placed for this reaction (Figures 4A and S1B), and serine 55 could provide hydrogen bonding stabilisation in this mechanism (Figure 5). This would explain why kynurenine is observed in the *Xc*TDO H55S structure, and L-Trp in the wild type.

In solution, the NFK product is released rapidly from the active site. So it is entirely possible that the formation of NFK and then kynurenine in the active site of H55S is a consequence of crystal lattice effects, which prevent the rapid release of NFK once formed. But the observation of kynurenine bound to the active site could still mean that TDO activity is inhibited in cases where kynurenine concentrations rise significantly. This raises the possibility that auto-regulatory mechanisms, dependent on kynurenine formation and re-binding to the enzyme, might also come into play in early steps of the pathway under certain conditions.

Declaration of Competing Interest

The authors declare that they have no known competing financial interests or personal relationships that could have appeared to influence the work reported in this paper.

Acknowledgments

We thank Professor Jonathan Clayden, University of Bristol, for helpful discussions on amide reactivity.

References

[1] E.L. Raven, J Biol Inorg Chem, vol. 22, 2017, pp. 175-183.
[2] I. Efimov, J. Basran, S.J. Thackray, S. Handa, C.G. Mowat, E.L. Raven, Biochemistry, vol. 50, 2011, pp. 2717-2724.
[3] J. Geng, A. Liu, Arch Biochem Biophys, vol. 544, 2014, pp. 18-26.

[4] D.A. Bender, Mol. Aspects Med., vol. 6, 1983, pp. 101-197.
[5] A.A.B. Badawy, Int J Tryptophan Res, vol. 10, SAGE Publications Ltd STM, 2017, pp. 1178646917691938.
[6] Y. Chen, G.J. Guillemin, Int J Tryptophan Res, vol. 2, Libertas Academica, 2009, pp. 1-19.
[7] M.D. Lovelace, B. Varney, G. Sundaram, N.F. Franco, M.L. Ng, S. Pai, C.K. Lim, G.J. Guillemin, B.J. Brew, Front. Immunol., vol. 7, Frontiers Media S.A., 2016, pp. 246-246.
[8] J.-P. Routy, B. Routy, G.M. Graziani, V. Mehraj, Int J Tryptophan Res, vol. 9, Libertas Academica, 2016, pp. 67-77.
[9] D.H. Munn, A.L. Mellor, Trends Immunol., vol. 37, 2016, pp. 193-207.
[10] F. Forouhar, J.L. Anderson, C.G. Mowat, S.M. Vorobiev, A. Hussain, M. Abashidze, C. Bruckmann, S.J. Thackray, J. Seetharaman, T. Tucker, R. Xiao, L.C. Ma, L. Zhao, T.B. Acton, G.T. Montelione, S.K. Chapman, L. Tong, Proc Natl Acad Sci U S A, vol. 104, 2007, pp. 473-478.
[11] S.J. Thackray, C. Bruckmann, J.L. Anderson, L.P. Campbell, R. Xiao, L. Zhao, C.G. Mowat, F. Forouhar, L. Tong, S.K. Chapman, Biochemistry, vol. 47, 2008, pp. 10677-10684.
[12] E.A. Berry, B.L. Trumpower, Anal. Biochem., vol. 161, 1987, pp. 1-15.
[13] M.M. Bradford, Anal. Biochem., vol. 72, 1976, pp. 248-254.
[14] S.J. Thackray, C. Bruckmann, J.L. Anderson, L.P. Campbell, R. Xiao, L. Zhao, C.G. Mowat, F. Forouhar, L. Tong, S.K. Chapman, Biochemistry, vol. 47, 2008, pp. 10677-10684.
[15] M.D. Winn, C.C. Ballard, K.D. Cowtan, E.J. Dodson, P. Emsley, P.R. Evans, R.M. Keegan, E.B. Krissinel, A.G.W. Leslie, A. McCoy, S.J. McNicholas, G.N. Murshudov, N.S. Pannu, E.A. Potterton, H.R. Powell, R.J. Read, A. Vagin, K.S. Wilson, Acta Crystallogr. Sect. D. Biol. Crystallogr., vol. 67, 2011, pp. 235-242.
[16] P.D. Adams, P.V. Afonine, G. Bunkoczi, V.B. Chen, I.W. Davis, N. Echols, J.J. Headd, L.-W. Hung, G.J. Kapral, R.W. Grosse-Kunstleve, A.J. McCoy, N.W. Moriarty, R. Oeffner, R.J. Read, D.C. Richardson, J.S. Richardson, T.C. Terwilliger, P.H. Zwart, Acta Crystallogr. Sect. D. Biol. Crystallogr., vol. 66, 2010, pp. 213-221.
[17] J. Basran, S.A. Rafice, N. Chauhan, I. Efimov, M.R. Cheesman, L. Ghamsari, E.L. Raven, Biochemistry, vol. 47, 2008, pp. 4752-4760.
[18] R.M. Davydov, N. Chauhan, S.J. Thackray, J.L. Anderson, N.D. Papadopoulou, C.G. Mowat, S.K. Chapman, E.L. Raven, B.M. Hoffman, J. Am. Chem. Soc., vol. 132, 2010, pp. 5494-5500.
[19] A. Lewis-Ballester, F. Forouhar, S.M. Kim, S. Lew, Y. Wang, S. Karkashon, J. Seetharaman, D. Batabyal, B.Y. Chiang, M. Hussain, M.A. Correia, S.R. Yeh, L. Tong, Sci Rep, vol. 6, 2016, pp. 35169.
[20] J. Geng, A.C. Weitz, K. Dornevil, M.P. Hendrich, A. Liu, Biochemistry, vol. 59, 2020, pp. 2813-2822.
[21] D. Batabyal, S.R. Yeh, J Am Chem Soc, vol. 129, 2007, pp. 15690-15701.
[22] J.S. Li, Q. Han, J.M. Fang, M. Rizzi, A.A. James, J.Y. Li, Archives of insect biochemistry and physiology, vol. 64, 2007, pp. 74-87.
[23] R. Fu, R. Gupta, J. Geng, K. Dornevil, S. Wang, Y. Zhang, M.P. Hendrich, A. Liu, J Biol Chem, vol. 286, 2011, pp. 26541-26554.
[24] L. Zhai, E. Ladomersky, A. Bell, C. Dussold, K. Cardoza, J. Qian, K.L. Lauing, D.A. Wainwright, Methods Enzymol, vol. 629, 2019, pp. 235-256.
[25] N. Yamasaki, T. Tsujita, F. Sakiyama, N. Masuda, Journal of biochemistry, vol. 80, 1976, pp. 1287-1292.
[26] B. Meng, D. Wu, J. Gu, S. Ouyang, W. Ding, Z.J. Liu, Proteins, vol. 82, 2014, pp. 3210-3216.
[27] K.N. Pham, A. Lewis-Ballester, S.R. Yeh, J Am Chem Soc, vol. 143, 2021, pp. 1836-1845.

[28] W. Huang, Z. Gong, J. Li, J. Ding, Journal of structural biology, vol. 181, 2013, pp. 291-299.
[29] Y. Zhang, S.A. Kang, T. Mukherjee, S. Bale, B.R. Crane, T.P. Begley, S.E. Ealick, Biochemistry, vol. 46, 2007, pp. 145-155.
[30] B.T. Parr, R. Pastor, B.D. Sellers, Z. Pei, F.A. Jaipuri, G.M. Castanedo, L. Gazzard, S. Kumar, X. Li, W. Liu, R. Mendonca, R.K. Pavana, H. Potturi, C. Shao, V. Velvadapu, J.P. Waldo, G. Wu, P.W. Yuen, Z. Zhang, Y. Zhang, S.F. Harris, A.J. Oh, A. DiPasquale, K. Dement, H. La, L. Goon, A. Gustafson, E.C. VanderPorten, M.R. Mautino, Y. Liu, ACS Med Chem Lett, vol. 11, 2020, pp. 541-549.
[31] M. Mirgaux, L. Leherte, J. Wouters, Acta Crystallogr D Struct Biol, vol. 76, 2020, pp. 1211-1221.
[32] M.T. Nelp, P.A. Kates, J.T. Hunt, J.A. Newitt, A. Balog, D. Maley, X. Zhu, L. Abell, A. Allentoff, R. Borzilleri, H.A. Lewis, Z. Lin, S.P. Seitz, C. Yan, J.T. Groves, Proc Natl Acad Sci U S A, vol. 115, 2018, pp. 3249-3254.
[33] S. Luo, K. Xu, S. Xiang, J. Chen, C. Chen, C. Guo, Y. Tong, L. Tong, Acta crystallographica. Section F, Structural biology communications, vol. 74, 2018, pp. 717-724.
[34] A. Lewis-Ballester, K.N. Pham, D. Batabyal, S. Karkashon, J.B. Bonanno, T.L. Poulos, S.R. Yeh, Nat Commun, vol. 8, 2017.
[35] A. Lewis-Ballester, S. Karkashon, D. Batabyal, T.L. Poulos, S.R. Yeh, J Am Chem Soc, vol. 140, 2018, pp. 8518-8525.
[36] C. White, M.A. McGowan, H. Zhou, N. Sciammetta, X. Fradera, J. Lim, E.M. Joshi, C. Andrews, E.B. Nickbarg, P. Cowley, S. Trewick, M. Augustin, K. von Koenig, C.A. Lesburg, K. Otte, I. Knemeyer, H. Woo, W. Yu, M. Cheng, P. Spacciapoli, P. Geda, X. Song, N. Smotrov, P. Curran, M.R. Heo, P. Abeywickrema, J.R. Miller, D.J. Bennett, Y. Han, ACS Med Chem Lett, vol. 11, 2020, pp. 550-557.
[37] Y.H. Peng, F.Y. Liao, C.T. Tseng, R. Kuppusamy, A.S. Li, C.H. Chen, Y.S. Fan, S.Y. Wang, M.H. Wu, C.C. Hsueh, J.Y. Chang, L.C. Lee, C. Shih, K.S. Shia, T.K. Yeh, M.S. Hung, C.C. Kuo, J.S. Song, S.Y. Wu, S.H. Ueng, Journal of medicinal chemistry, vol. 63, 2020, pp. 1642-1659.
[38] H. Zhang, K. Liu, Q. Pu, A. Achab, M.J. Ardolino, M. Cheng, Y. Deng, A.C. Doty, H. Ferguson, X. Fradera, I. Knemeyer, R. Kurukulasuriya, Y.H. Lam, C.A. Lesburg, T.A. Martinot, M.A. McGowan, J.R. Miller, K. Otte, P.J. Biju, N. Sciammetta, N. Solban, W. Yu, H. Zhou, X. Wang, D.J. Bennett, Y. Han, ACS Med Chem Lett, vol. 10, 2019, pp. 1530-1536.
[39] U.F. Rohrig, A. Reynaud, S.R. Majjigapu, P. Vogel, F. Pojer, V. Zoete, Journal of medicinal chemistry, vol. 62, 2019, pp. 8784-8795.
[40] S. Kumar, J.P. Waldo, F.A. Jaipuri, A. Marcinowicz, C. Van Allen, J. Adams, T. Kesharwani, X. Zhang, R. Metz, A.J. Oh, S.F. Harris, M.R. Mautino, Journal of medicinal chemistry, vol. 62, 2019, pp. 6705-6733.
[41] K.N. Pham, S.R. Yeh, J Am Chem Soc, vol. 140, 2018, pp. 14538-14541.
[42] S. Crosignani, P. Bingham, P. Bottemanne, H. Cannelle, S. Cauwenberghs, M. Cordonnier, D. Dalvie, F. Deroose, J.L. Feng, B. Gomes, S. Greasley, S.E. Kaiser, M. Kraus, M. Negrerie, K. Maegley, N. Miller, B.W. Murray, M. Schneider, J. Soloweij, A.E. Stewart, J. Tumang, V.R. Torti, B. Van Den Eynde, M. Wythes, Journal of medicinal chemistry, vol. 60, 2017, pp. 9617-9629.
[43] J.A.C. Alexandre, M.K. Swan, M.J. Latchem, D. Boyall, J.R. Pollard, S.W. Hughes, J. Westcott, Chembiochem : a European journal of chemical biology, vol. 19, 2018, pp. 552-561.
[44] Y. Wu, T. Xu, J. Liu, K. Ding, J. Xu, Biochem Biophys Res Commun, vol. 487, 2017, pp. 339-343.

[45] Y.H. Peng, S.H. Ueng, C.T. Tseng, M.S. Hung, J.S. Song, J.S. Wu, F.Y. Liao, Y.S. Fan, M.H. Wu, W.C. Hsiao, C.C. Hsueh, S.Y. Lin, C.Y. Cheng, C.H. Tu, L.C. Lee, M.F. Cheng, K.S. Shia, C. Shih, S.Y. Wu, Journal of medicinal chemistry, vol. 59, 2016, pp. 282-293.
[46] S. Tojo, T. Kohno, T. Tanaka, S. Kamioka, Y. Ota, T. Ishii, K. Kamimoto, S. Asano, Y. Isobe, ACS Med Chem Lett, vol. 5, 2014, pp. 1119-1123.
[47] Q. Pu, H. Zhang, L. Guo, M. Cheng, A.C. Doty, H. Ferguson, X. Fradera, C.A. Lesburg, M.A. McGowan, J.R. Miller, P. Geda, X. Song, K. Otte, N. Sciammetta, N. Solban, W. Yu, D.L. Sloman, H. Zhou, A. Lammens, L. Neumann, D.J. Bennett, A. Pasternak, Y. Han, ACS Med Chem Lett, vol. 11, 2020, pp. 1548-1554.

Figure legends

Figure 1. Heme dioxygenases such as TDO and IDO catalyse the oxidation of L-tryptophan to N-formylkynurenine (NFK). Hydrolysis of NFK by the kynurenine formamidase enzyme leads to formation of L-kynurenine.

Figure 2. Crystal structure of *Xc*TDO H55S in complex with L-kynurenine. (A) Electron density map showing the binding of L-kynurenine (Kyn) and the CN^- ligand bound to the iron. Note that cyanide is bound in six out of eight molecules in the unit cell, with water coordinated to the iron in the other two molecules. (B) The same as in (A), but showing hydrogen bonding interactions to the protein (yellow dashed lines). (C) Overall structure of the *Xc*TDO H55S structure showing the flexible loop (residues 250 - 260) highlighted in orange and one Trp per monomer bound at the interface.

Figure 3. (A) Oxidation of L-Trp by ferric *Xc*TDO. (B) Oxidation of L-Trp by ferric *Xc*TDO H55S. In (A) and (B) the spectral changes shown are observed upon reaction with L-Trp (2 mM) for 60 min under atmospheric conditions. (C) Oxidation of L-Trp by ferric *Xc*TDO H55S under anaerobic conditions. The spectral changes shown are observed upon reaction of ferric *Xc*TDO H55S with L-Trp (2 mM) under anaerobic conditions for 180 min. No increase in absorbance at 321 nm is observed. (D) Oxidation of L-Trp by ferric *Xc*TDO in the presence of 5mM KCN. Spectral changes shown are observed upon reaction of ferric *Xc*TDO with L-Trp (2 mM) under aerobic conditions. Spectra were recorded at time points t = 0, 60, 120, 180, 300 min. No substantial changes in absorbance at 321 nm were observed over these timescales in an equivalent experiment using *Xc*TDO H55S, probably because of the overall lower activity of this variant towards L-Trp in the first place. In all cases arrows indicate the direction of the absorbance change. Reaction conditions: 50 mM Tris-HCl, pH 8.0, 25.0 °C.

Figure 4. Comparison of L-kynurenine, L-Trp and NFK binding orientations. (A) The structure of *Xc*TDO H55S with kynurenine bound (shown in beige), overlaid with the structures of wild type *Xc*TDO in complex with L-Trp (cyan, 2NW8) and *Xc*TDO H55S in complex with L-Trp (green, 3E08). The water molecule labelled * is the same one as referred to in Figure 5 and Figure S1A,B. (B) Comparison of L-kynurenine and NFK binding orientations. Structure of *Xc*TDO H55S with L-kynurenine bound (beige) overlaid with the structure of wild type human TDO in complex with NFK (orange, 5TI9). Water molecules are shown as spheres, in the same colours as the respective structures.

Figure 5. Possible mechanism of NFK hydrolysis, leading to formation of L-kynurenine. Formation of NFK in the ferric TDO enzyme (either wild type or H55S) leads to NFK. The H^+-dependent hydrolysis of the amide group in NFK occurs readily and has chemical precedent [25]. Serine 55 is well positioned (see Figure 4A) to provide hydrogen bonding stabilisation in this proton-catalysed mechanism. The active site water molecule hydrogen bonded to serine 55

(labelled * in Figure 4 and Figure S1) appears also to be well positioned, but other water molecules in the active site (*e.g.* H_2O bound to iron) might also be candidates. Other mechanisms are feasible, see Figure S4. The involvement of serine 55 in the active site led us to consider the possibility of amide hydrolysis occurring in a manner similar to a serine protease, however from the structure there are no suitably positioned His or and Asp/Glu residues to form a catalytic triad.

Table 1
Data collection and refinement statistics.

Data Collection	
Resolution (Å)	117.75 – 1.70 (1.79 – 1.70)
Total measured reflections	990829
Unique reflections	268120 (34391)
Completeness (%)	97.9 (86.5)
Redundancy	3.7 (3.0)
I/σ (I)	13.4 (2.9)
Unit cell dimensions (Å)	a=78.1, b=117.7, c=138.8
Space group	P 121
R_{merge}	0.055 (0.342)
Refinement	
R_{work}/R_{free}	0.14/0.18
r.m.s.d. bond (Å)/angle (°)	0.014/1.0
Ramachandran analysis	
Most favoured (%)	98.5
Allowed (%)	1.4
Outliers (%)	0.1

Table 2
Summary of IDO and TDO crystal structures from the Protein Data Bank.

TDO	Oxidation state / complex	PDB code	Ref
X. campestris TDO	Ferric	2NW7	[10]
X. campestris TDO	Ferric	1YW0	Unpublished
X. campestris TDO	Ferrous / Trp	2NW8	[10]
X. campestris TDO H55S	Ferric / Trp	3E08	[11]
X. campestris TDO H55A	Ferric / Trp	3BK9	[11]
X. campestris TDO H55S	Ferric / NFK / CN	7P46	This work
Human TDO	Ferric	4PW8	[26]
Human TDO	Ferric / Trp	5TIA	[19]
Human TDO	Ferrous / Trp / O_2	5TI9	[19]
	Ferric / NFK	5TI9	[19]
Human TDO	Ferrous / Trp / CO	6UD5	[27]
Drosophilia TDO	Ferric	4HKA	[28]
R. metallidurans TDO	Ferric	2NOX	[29]
Human TDO / inhibitor	Ferric	6PYZ, 6PYY	[27]
Human TDO / inhibitor	Ferric[a]	6A4I	unpublished
Human TDO-2 / inhibitor	Ferric	6VBN	[30]

IDO	Oxidation state / complex	PDB code	Ref
Human IDO	Ferric	7A62	[31]
Human IDO	Ferric	6AZU	[32]
Human IDO	Ferric	6E44	[33]
Human IDO	Ferrous	6E45	[33]
Human IDO	Ferrous / Trp	6E46	[33]
Human IDO	Ferric / Trp / CN[a]	6E35	Unpublished
Human IDO	Ferric / Trp / CN	5WMU, 5WMW (F270G)	[34]
Human IDO (S167H)	Ferric / Trp / CN Ferric/ Trp / CN / Inhibitor	6CXU, 6CXV	[35]
Human IDO / Trp / CO	Ferrous / Trp / CO	6UBP	[27]
Human IDO / inhibitor	Ferric[a]	6V52	[36]
Human IDO / inhibitor	Ferric[a]	6KW7, 6KOF, 6KPS	[37]
Human IDO / inhibitor	Ferric[a]	6PZ1	[27]
Human IDO / inhibitor	Ferric[a]	6PU7	[38]
Human IDO / inhibitor	Ferric[a]	6R63	[39]
Human IDO / inhibitor	Ferric[a]	6O3I	[40]
Human IDO / inhibitor	Ferric[a]	6E43, 6E42, 6E41, 6E40	[33]
Human IDO / inhibitor	Ferric[a]	6DPR, 6DPQ, 6MQ6	[41]
Human IDO / inhibitor	Ferric[a]	6AZW, 6AZV	[32]
Human IDO / inhibitor	Ferric[a]	5WHR	[42]
Human IDO / inhibitor	Ferric[a]	6F0A	[43]
Human IDO / inhibitor	Ferric / Trp / CN	5WMX (F270G) 5WN8, 5WMV	[34]
Human IDO / inhibitor	Ferric[a]	5XE1	[44]
Human IDO / inhibitor	Ferric[a]	5ETW, 5EK4, 5EK3, 5EK2	[45]
Human IDO / inhibitor	Ferric[a]	4PK5, 4PK6	[46]
Human IDO / inhibitor	Ferric[a]	6WJY	[47]
Human IDO A260G & G262A	4-phenylimidazole	4U72, 4U74	Unpublished

[a] Presumed ferric oxidation state, but not stated.

Figure 1

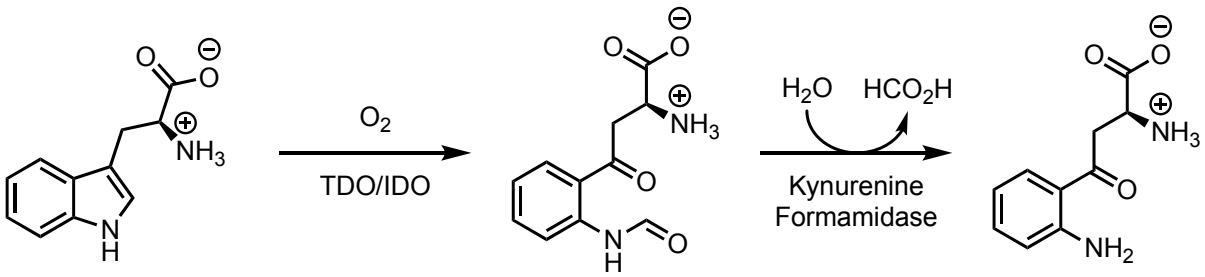

L-Tryptophan **_N_-formylkynurenine** **L-Kynurenine**

Figure 2

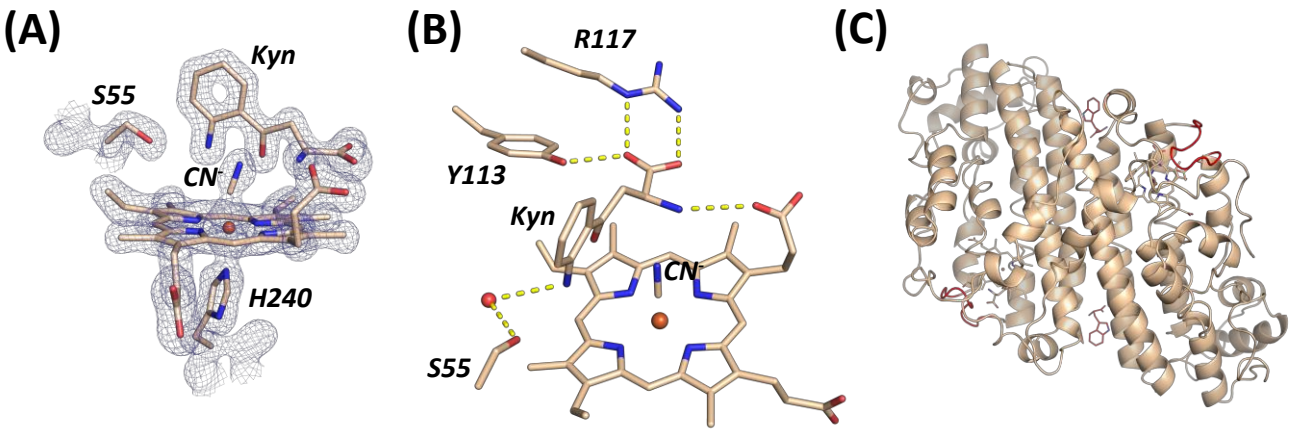

Figure 3

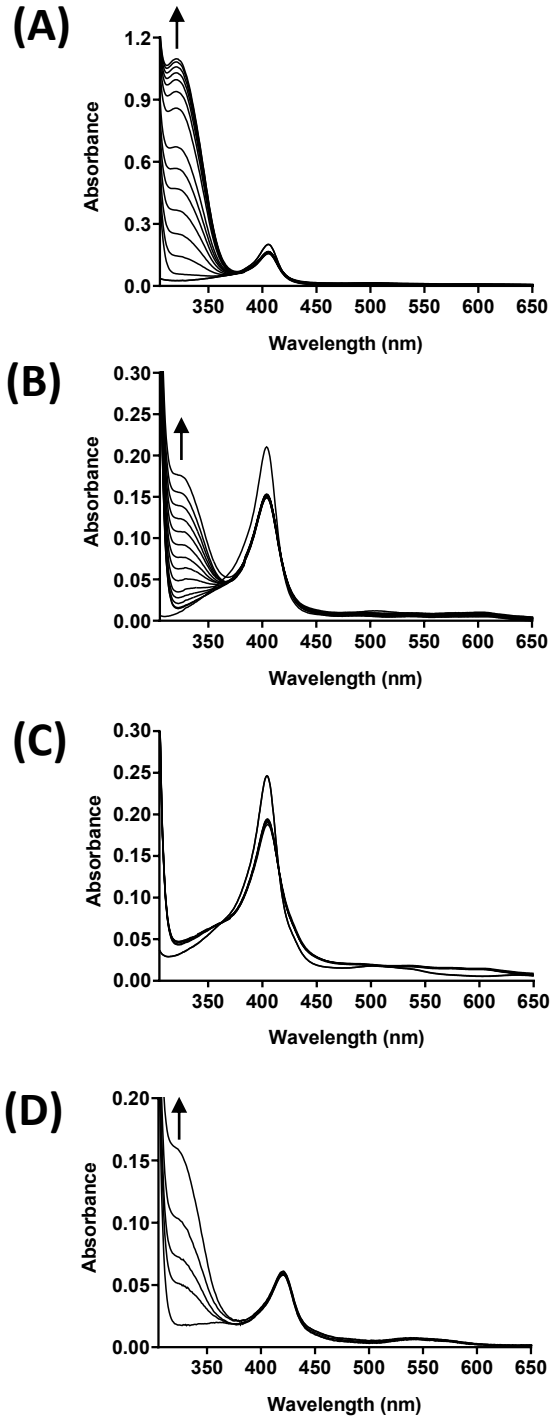
(A)
Absorbance
1.2
0.9
0.6
0.3
0.0
350 400 450 500 550 600 650
Wavelength (nm)
(B)
Absorbance
0.30
0.25
0.20
0.15
0.10
0.05
0.00
350 400 450 500 550 600 650
Wavelength (nm)
(C)
Absorbance
0.30
0.25
0.20
0.15
0.10
0.05
0.00
350 400 450 500 550 600 650
Wavelength (nm)
(D)
Absorbance
0.20
0.15
0.10
0.05
0.00
350 400 450 500 550 600 650
Wavelength (nm)

Figure 4

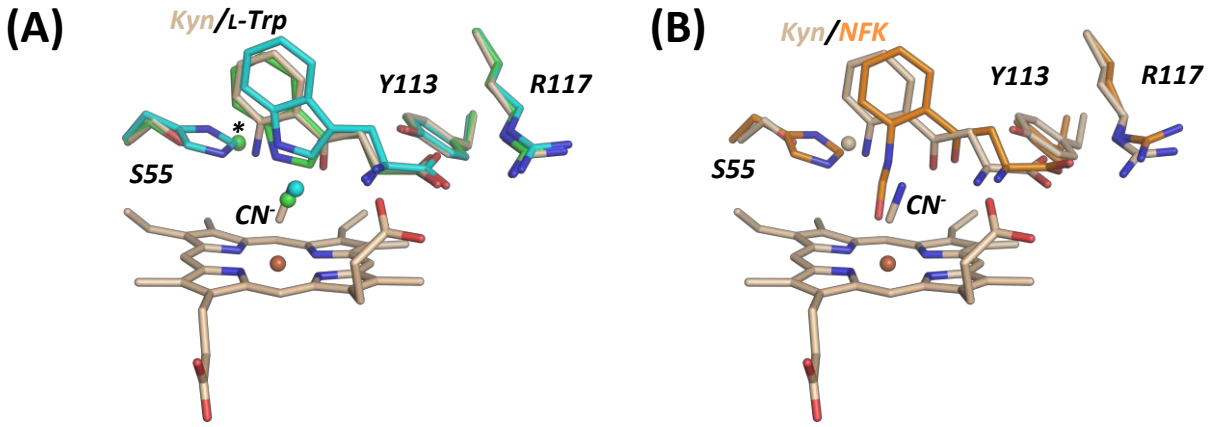

Figure 5

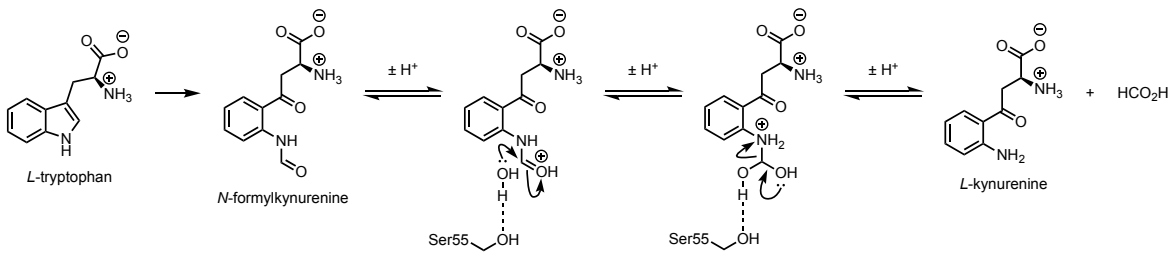
L-tryptophan
N-formylkynurenine
± H+
± H+
± H+
Ser55
Ser55
L-kynurenine
+ HCO2H

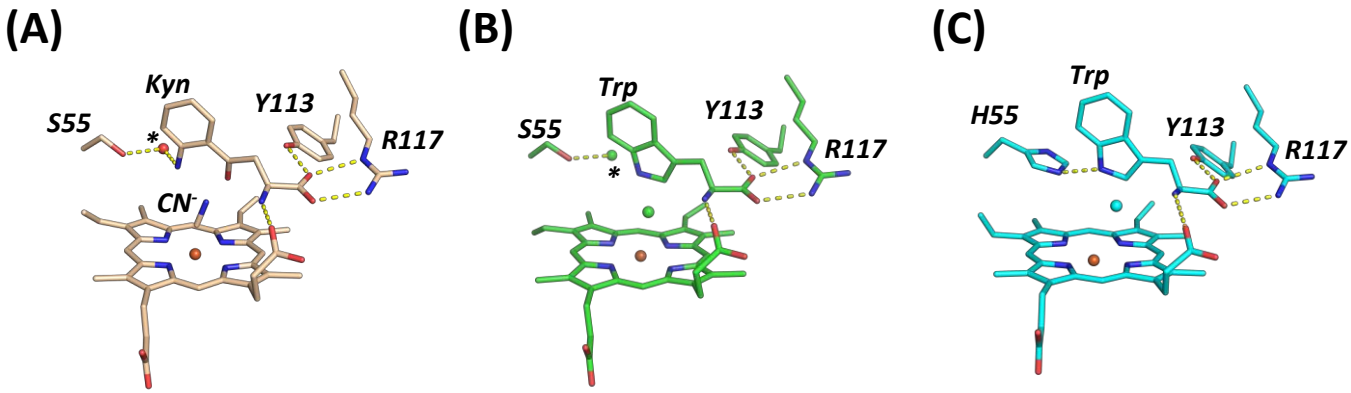

Figure S1. Comparison of the hydrogen bonding interactions involved in binding (A) L-kynurenine and (B) L-Trp to *Xc*TDO H55S (PDB 3E08). A water molecule (labelled *) at ~2.8 Å from Ser55 is conserved in both structures and could be involved in hydrolysis (see Figure 5). In (C) is shown the structure of wild type *Xc*TDO in complex with L-Trp (2NW7).

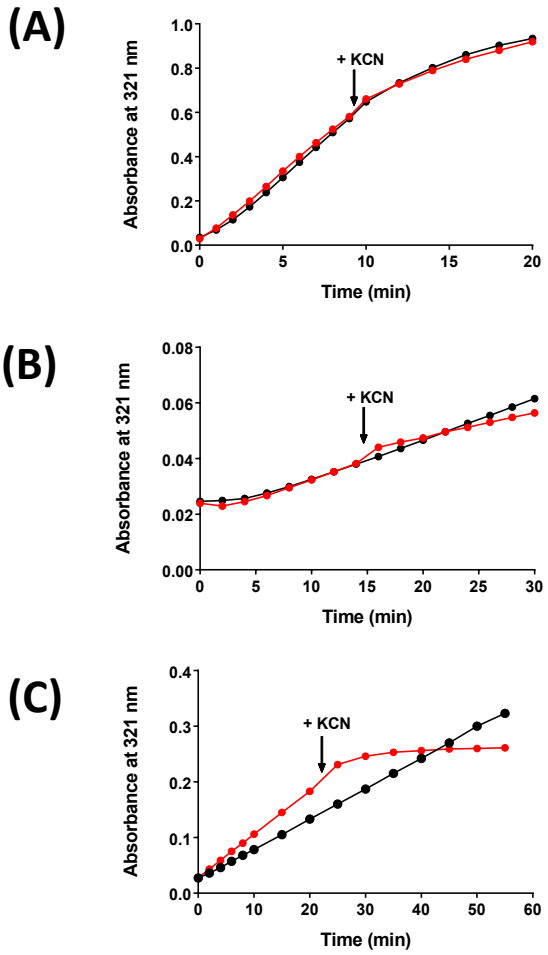

Figure S2. Effect of KCN on the rate of NFK formation observed at A_{321} nm for the reaction catalysed by (A) *Xc*TDO, (B) *Xc*TDO H55S and (C) human TDO. Addition of 1mM KCN to the reaction mix is indicated by the arrow in each figure. Reaction conditions: 50 mM Tris-HCl, pH 8.0, 25.0 °C

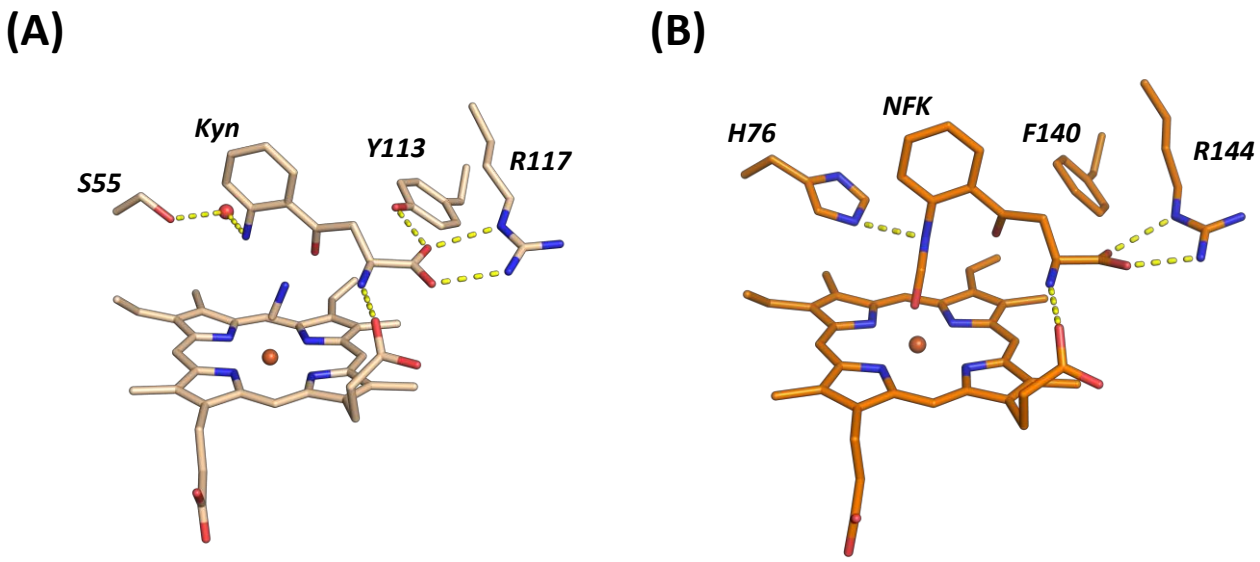

Figure S3. Comparison of the hydrogen bonding interactions involved in binding (A) L-kynurenine to *Xc*TDO H55S and (B) NFK to human TDO (PDB 5TI9).

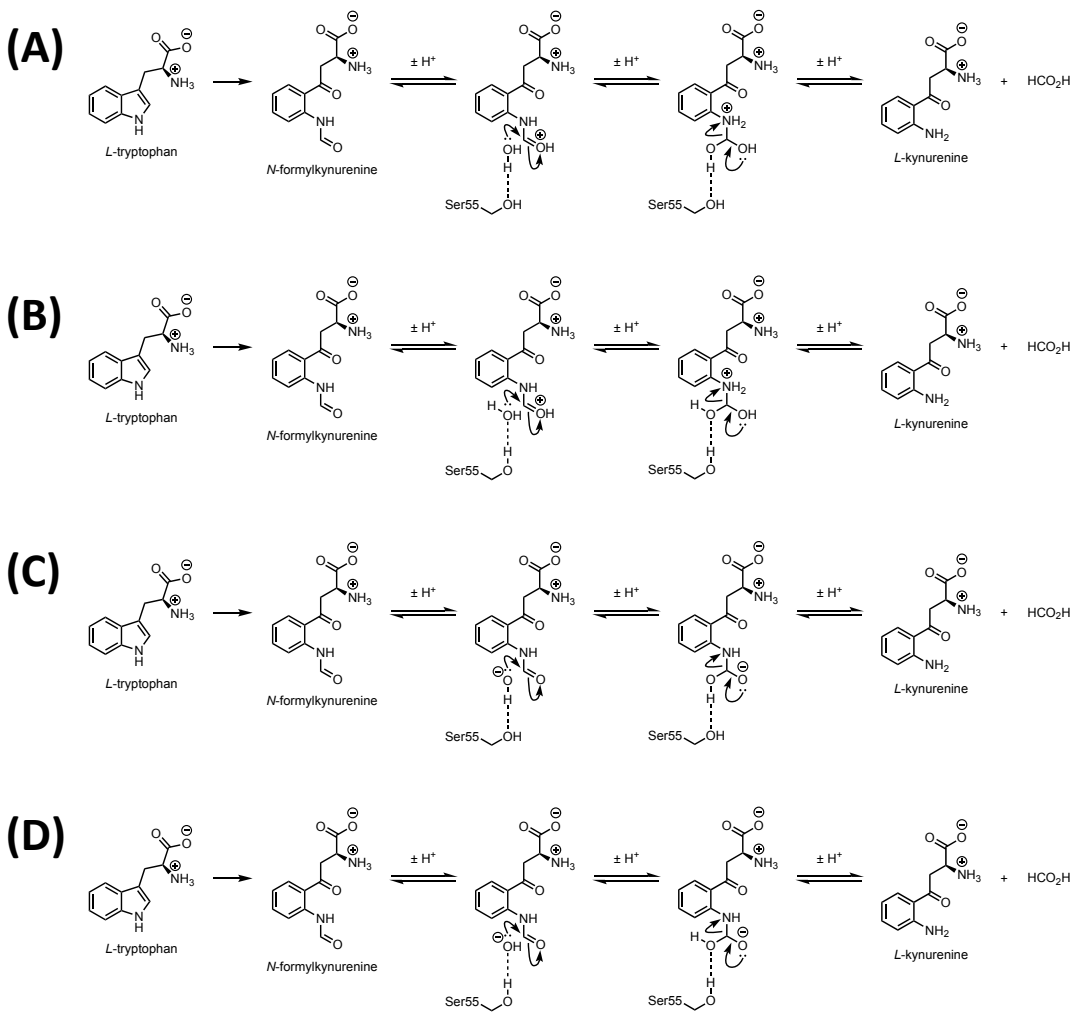

Figure S4. We envisage numerous possible mechanisms for NFK hydrolysis. In (A) is shown the same acid-catalysed mechanism as in Figure 5. (B) An alternative version of this acid-catalysed mechanism, using different hydrogen bonds to serine 55. (C) and (D) show an equivalent base-catalysed mechanism. We cannot distinguish these mechanisms in our structures.

Graphical abstract

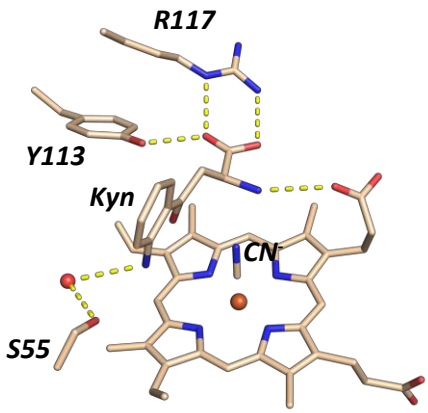

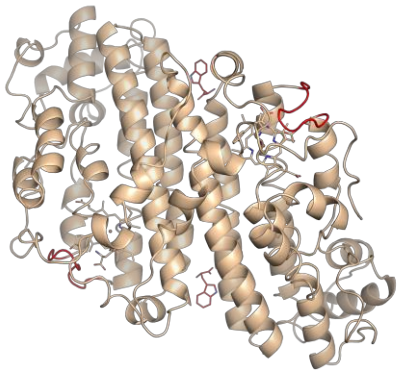

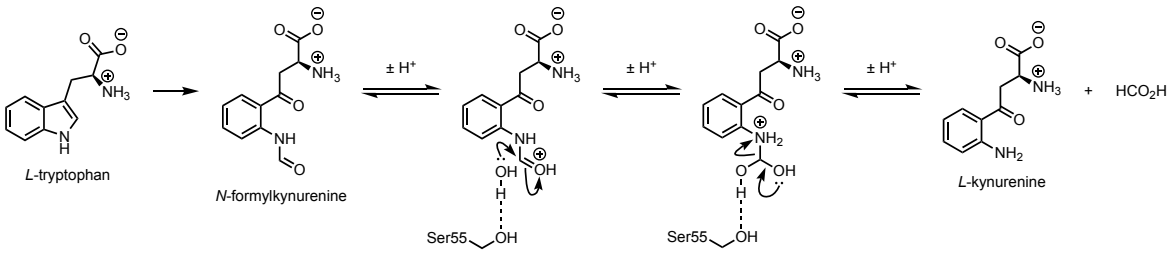

Declaration of interests

☒ The authors declare that they have no known competing financial interests or personal relationships that could have appeared to influence the work reported in this paper.

☐The authors declare the following financial interests/personal relationships which may be considered as potential competing interests:

Author contributions

H.K., C.G.M. and E.L.R. designed the research; J.B., E.S.B, L.P.C., S.J.T., M.H.J. and H.K. performed the experiments; all authors analysed and interpreted data; E.L.R wrote the paper with contributions from all authors.